In-situ control of oxygen fugacity for laboratory measurements of electrical conductivity of minerals and rocks in a multi-anvil press*

Dai Li-Dong(代立东)[a], Li He-Ping(李和平)[a]†, Hu Hai-Ying(胡海英)[a,b], and Shan Shuang-Ming(单双明)[a]

[a] *Laboratory for Study of the Earth's Interior and Geofluids, Institute of Geochemistry, Chinese Academy of Sciences, Guiyang* 550002, *China*

[b] *Graduate School of the Chinese Academy of Sciences, Beijing* 100049, *China*

(Received 3 November 2010; revised manuscript received 3 December 2010)

In this paper, a new of oxygen fugacity controltechnique that can be widely applied to *in-situ* measurement of the grain interior electrical conductivities of minerals and rocks is presented for high temperature and high pressure. Inside the sample assembly, a metal and corresponding metal oxide form a solid oxygen buffer. The principle of this technique is to randomly monitor and adjust oxygen fugacity in the large-volume multi-anvil press by changing the types of solid oxygen buffer, metal shielding case and electrodes. At a pressure of up to 5.0 GPa and a temperature of up to 1423 K, the electrical conductivities of the dry peridotite are tested under the conditions of different oxygen fugacities. By virtue of this new technique, more and more reasonable and accurate laboratory electrical property data will be successfully obtained under controlled thermodynamic conditions.

Keywords: oxygen fugacity, electrical conductivity, large-volume multi-anvil press

PACS: 91.25.F–, 91.35.Gf, 91.60.Pn **DOI:** 10.1088/1674-1056/20/4/049101

1. Introduction

Under controlled thermodynamic conditions, the *in-situ* laboratory measurement of the electrical conductivities of minerals and rocks at high temperature and high pressure is the most straightforward and efficient means to explore their composition, characteristics and state of the materials in the Earth's interior. The electrical properties of minerals and rocks can also provide crucial information about the structure of the Earth's interior, the migration process of electrons and ions, the point defect chemistry, thermoelectric coefficient and phase transition.[1−12]

Oxygen fugacity is a key parameter in the petrogenesis and it is necessary to control the oxygen fugacity in experimental mineralogy, petrology and geochemistry.[13−20] Currently, oxygen fugacity and water content are two dominant research hotspots in the electrical conductivity measurements of minerals and rocks at high temperatures and pressures.[21−25] We have recently developed a new technique of controlling oxygen fugacity during high-pressure measurements of the electrical conductivities of minerals and rock in the YJ-3000t in the Laboratory for Study of the Earth's Interior and Geofluids of the Institute of Geochemistry, Chinese Academy of Sciences, and Kawai-1000t in the Department of Geology and Geophysics, Yale University, which has been widely applied to the large volume multi-anvil high-pressure press. Furthermore, we have already succeeded in carrying out *in-situ* measurements of the electrical conductivities of single crystal olivine, single crystal pyroxene, pyrope garnet, peridotite, pyroxenite, lherzolite and wadsleyite, which are dominant and abundant minerals and rocks in the upper mantle and transition zone.[3−9,24,25] Will and his collaborators[26] succeeded in measuring the electrical conductivities of synthetic Ni_2SiO_4, Fe_2SiO_4 and $MgSiO_3$, where the the single frequency AC method was adopted ($V = 5.4 \times 10^{-3}$ V–5.4 V and 1.6 kHz) under the conditions of 2.0 GPa, 613 K–1373 K and two solid oxy-

*Project supported by the Knowledge Innovation Key Orientation Project of the Chinese Academy of Sciences (CAS) (Grant Nos. KZCX2-YW-Q08-3-4, KZCX2-YW-QN110, and KZCX3-SW-124), Large-scale Scientific Apparatus Development Program of CAS (Grant No. YZ200720), the National High Technology Research and Development Program of China (Grant No. 2006AA09Z205), and the National Natural Science Foundation of China (Grant Nos. 40974051, 40704010 and 40573046).

†Corresponding author. E-mail: hepingli_2007@hotmail.com

© 2011 Chinese Physical Society and IOP Publishing Ltd

gen buffers of FQM (Fayalite+Quartz+Magnetite)-FQI (Fayalite+Quartz+Iron). Xu *et al.*[27] used the AC impedance spectroscopic method and the Mo–MoO_2 single solid buffer controlling oxygen fugacity to successfully obtain the electrical conductivities of olivine and its high-pressure polymorph, it is the first time that we have adopted the different solid buffers to realize the different oxygen fugacities during the measurements of grain interior and grain boundary electrical properties of minerals and rocks at high temperature and high pressure. Although Dai *et al.*[4] have already measured the grain boundary electrical conductivity of dry mantle peridotite under conditions of 1.0 GPa–4.0 GPa, 1073 K–1423 K, the frequency ranging from 10^{-2} Hz to 10^3 Hz and controlling oxygen fugacities, till now, there is not any report dealing with the measurement of the grain interior electrical conductivity under conditions of higher pressure, wider frequency range, and controlled thermodynamics.

In the present work, we measure the grain interior electrical conductivity of the dry peridotite under conditions of 5.0 GPa, 1423 K and the frequency ranging from 10^2 Hz to 10^6 Hz. According to the order from the reducibility to oxidizability, five solid oxygen buffers including Mo+MoO_2 (MMO), Fe+FeO (IW), Fe+Fe_3O_4 (IM), Ni+NiO (NNO), and Fe_2O_3+Fe_3O_4 (MH) are sequentially chosen so as to control the oxygen partial pressure. Then, a relationship that describes the electrical conductivity and oxygen fugacity independent of temperature and pressure is successfully established at high temperature and high pressure. Therefore, by changing the types of the metal and corresponding metal oxide, the oxygen fugacity is efficiently controlled during the grain interior electrical conductivity measurement.

2. Experimental procedures

The experiments were all performed by using the YJ-3000t multi-anvil large volume high-pressure apparatus in the Laboratory for Study of the Earth's Interior and Geofluids, Institute of Geochemistry, Chinese Academy of Sciences, China. For the detailed description of the equipment, please refer to the papers by Xie *et al.*[28] and Li *et al.*[29] All the observations including the transmission electron microscope, microstructure analysis, infrared spectrum and Raman spectrum were conducted in the Department of Geology and Geophysics, Yale University, USA and Department of Earth and Planetary Sciences, Tokyo Institute of Technology, Japan. The experimental assembly is shown in Fig. 1. The detailed experimental procedures have already been presented by Dai *et al.*,[4] where the grain boundary electrical conductivity of dry peridotite was measured. Here, we focus our attention mainly on elaborating the experimental principle of controlling oxygen fugacity.

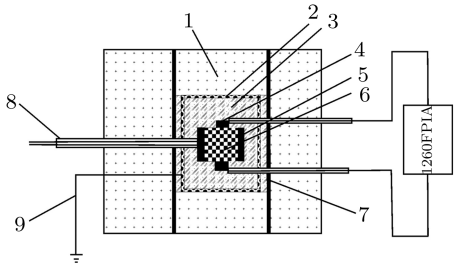


Fig. 1. Sample assembly for controlling oxygen fugacity. 1: Pyrophyllite; 2: metal shielding cases; 3: alumina; 4: electrode; 5: solid buffer tube; 6: sample; 7: tri-layers stainless steel heater; 8: Pt–$PtRh_{10}$ thermocouple; 9: earth line.

Several ordinary different kinds of high-purity powders of metals (e.g. Ni, Fe, and Mo) and their corresponding metal oxides (e.g. NiO, FeO, Fe_2O_3, Fe_3O_4, and MoO_2) were selected and mechanically mixed correspondingly. The ratios of metals and metal oxides were adopted according to the weight percentages that were shown by the following buffer equations of chemical reaction:

$$\mathrm{NNO}: \ 2\mathrm{Ni} + \mathrm{O_2} \rightleftharpoons 2\mathrm{NiO}, \tag{1}$$

$$\mathrm{MH}: \ 4\mathrm{Fe_3O_4} + \mathrm{O_2} \rightleftharpoons 6\mathrm{Fe_2O_3}, \tag{2}$$

$$\mathrm{IM}: \ 3\mathrm{Fe} + 2\mathrm{O_2} \rightleftharpoons \mathrm{Fe_3O_4}, \tag{3}$$

$$\mathrm{IW}: \ 2\mathrm{Fe} + \mathrm{O_2} \rightleftharpoons 2\mathrm{FeO}, \tag{4}$$

$$\mathrm{MMO}: \ \mathrm{Mo} + \mathrm{O_2} \rightleftharpoons \mathrm{MoO_2}. \tag{5}$$

Under conditions of $P = 133$ MPa, $T = 1573$ K and argon gas as a pressure medium in the China Iron & Steel Research Institute, solid oxygen buffers were pressed tightly and sintered, then we obtained the electrode slices and buffer loops that were cut and polished from the recovery blocks of sold oxygen buffers by the technique of electric spark discharge and erosion.

For the each sold buffer, oxygen fugacity values are a function of pressure and temperature which can be expressed by the following relation:[30]

$$\log f_{\mathrm{O_2}} = -\frac{\alpha}{T} + \beta + \gamma\frac{(P-1)}{T}, \tag{6}$$

where α, β and γ are constants directly related to the standard enthalpy, the standard entropy, and the molar volume variation of the solid ingredients before and after the buffering chemical balance reaction; T is the absolute temperature (K), and P is the pressure (Pa).

Based on the sequence from reducibility to oxidizability, we make a theoretical calculation and obtain the parameter values of each solid oxygen buffer as follows: MMO: $\alpha = 30650$, $\beta = 8.92$ and $\gamma = 0.054$; IW: $\alpha = 27215$, $\beta = 6.57$ and $\gamma = 0.052$; IM: $\alpha = 29260$, $\beta = 8.99$ and $\gamma = 0.061$; NNO: $\alpha = 24930$, $\beta = 9.36$ and $\gamma = 0.046$, and MH: $\alpha = 24634$, $\beta = 13.97$ and $\gamma = 0.019$. In this work, the oxygen fugacity is demonstrated to be true by changing the metal-bearing types in the shielding case, electrodes and the corresponding buffer loop type at a given temperature and pressure. In addition, to verify the efficiency and the accuracy of the solid oxygen buffer, it is crucial to perform the x-ray diffraction analysis on the recovery buffers after electrical conductivity measurements. If two-phase coexistence is available for each metal and metal oxide, the oxygen fugacity is effectively controlled.

3. Results and discussion

In order to check the validity and efficiency of controlling method, under conditions of 5.0 GPa, 1423 K and the frequency ranging from 10^2 Hz to 10^6 Hz, we have performed the *in-situ* measurement of the grain interior electrical conductivity of the dry synthetic peridotite which originates from the Han Nuoba area, Zhangjiakou city, Hebei Province, China. According to the sequence from oxidizability to reducibility, five solid buffers (MH, NNO, IM, IW and MMO) are used to control the oxygen partial pressure.

The representative impedance spectroscopic curves for the dry synthetic peridotite are shown in Figs. 2–5. The Solartron-1260 Impedance/Gain-Phase Analyzer with a 1.0-V signal voltage and the fixed frequency raging from 10^2 Hz to 10^6 Hz is employed to measure the complex impedance of samples. Figure 2 shows the Nyquist (Cole–Cole) diagram indicating the relationship between real component (Z') and imaginary component (Z'') of the complex impedance. Figures 3–5 show the Bode diagrams representing the dependences of real component (ReZ), imaginary component (ImZ), magnitude ($|Z|$), and the phase angle (Φ) on the frequency of the complex impedance. According to Long *et al.*,[31,32] under controlled the frequency ranging from 10^2 Hz to 10^6 Hz, there appears the grain interior process only in a single conduction mechanism. The semi-circle diameter of the impedance spectroscopy represents the resistance of sample. With the increase of oxygen fugacity, the semi-circle arc becomes smaller and smaller, and therefore the resistance value of the sample gradually decreases. As shown in Bode Figs. 2–5, there is a regular change between the real component, imaginary component, magnitude and phase angle with the frequency. With the decrease of frequency from 10^6 Hz to 10^2 Hz, (i) the real component and the magnitude of the sample quickly rise, and then they gradually tend to the approximately fixed values, (ii) the imaginary component reaches the peak value where the frequency is approximate to 10^3 Hz$\sim 10^4$ Hz, and then it gradually tends to a fixed value, (iii) the phase angle quickly rises, and then it gradually tends to a fixed value.

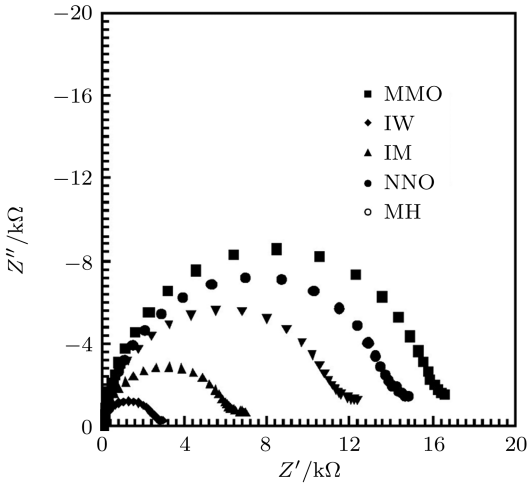


Fig. 2. Curves for Nyquist of complex impedance of Z' versus Z'' for dry peridotite from 10^2 Hz–10^6 Hz (from right to left), obtained under the conditions of 5.0 GPa, 1423 K and five different solid buffers (MMO, IW, IM, NNO and MH). Z' and Z'' denote the real and the imaginary components of complex impedance, respectively.

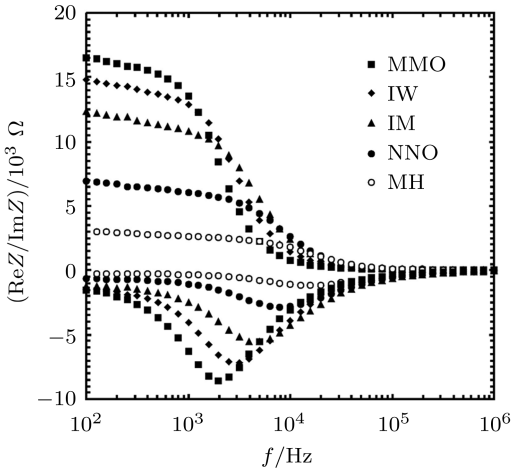


Fig. 3. Dependences of the real component (ReZ) and the imaginary component (ImZ) of the complex impedance of dry peridotite on frequency under the conditions of 5.0 GPa, 1423 K and different solid buffers. The frequencies at which the individual data were measured decrease from left to right.

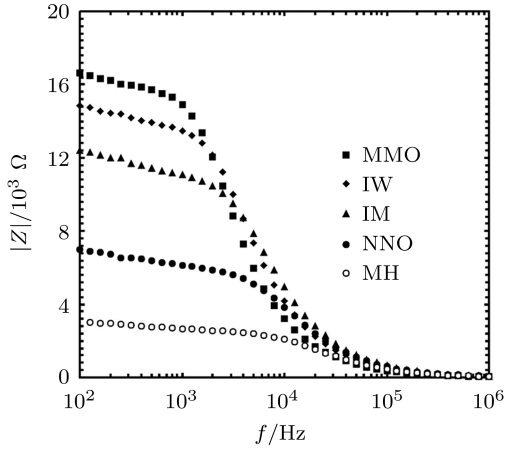


Fig. 4. Dependences of the magnitude, $|Z|$, of the complex impedance of dry peridotite on frequency under the conditions of 5.0 GPa, 1423 K and different solid buffers.

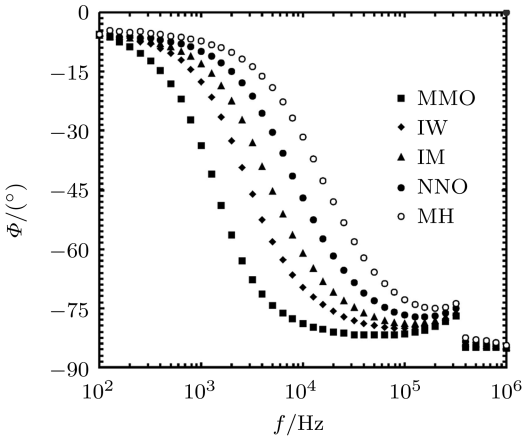


Fig. 5. Dependences of the phase angle, Φ, of the complex impedance of dry peridotite on frequency under the conditions of 5.0 GPa, 1423 K and different solid buffers.

The grain interior electrical conductivity of dry synthetic peridotite can be determined through the following equation:

$$\sigma = \frac{L/S}{R} = \frac{L}{SR}, \tag{7}$$

where L is the length of the sample, S is the sectional area of the electrode, and R is the resistance of the sample.

Figure 6 shows the relationship between the grain interior electrical conductivity of the dry synthetic peridotite and oxygen fugacity under controlled MH, NNO, IM, IW and MMO five solid oxygen buffers. Based on the logarithmic diagram unit, we find that the electrical conductivity of the sample increases with the rise of the oxygen fugacity and there exists a good linear relation. The oxygen fugacity value of the reduction boundary (MMO) and oxidation boundary (MH) of the selected solid oxygen buffer has only 10^9 order of magnitude variation, which results in the better linear correlation coefficient value ($R^2 = 0.99$).

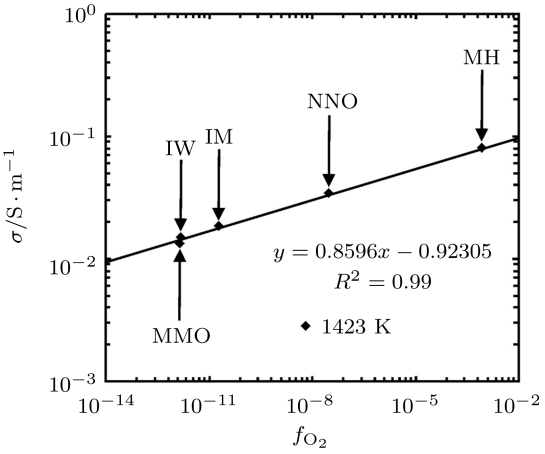


Fig. 6. Relationship between the grain interior electrical conductivity and oxygen fugacity under the conditions of 5.0 GPa and 1423 K.

It is common sense that the oxidation state of the upper mantle lies in a range from IW (Fe+FeO) to FQM (Fayalite+Quartz+Magnetite close to NNO) buffers.[33] Therefore, in this paper, the oxygen buffer value that we chose the solid metal and metal oxide to monitor can be suited for completely indicating the thermodynamic environments of minerals and rocks in the upper mantle. We execute the non-linear advanced fitting program in the ORIGIN software, and perform the complex non-linear least square fitting with the Levenberg–Marquardt iterative method at least 100 times and the error analysis according to the non-linear least square principle.[34] In this way, the relationship model (8) of the electrical conductivity and oxygen fugacity is successfully obtained, and the fitting result error is less than 4%.

The x-ray diffraction recovery oxygen buffer after each experiment of electrical conductivity measurement must be checked by two-phase coexistence analysis in order to confirm the efficiency and the accuracy of the oxygen buffer. A new laboratory-based model representing the relationship between grain interior electrical conductivity of the dry synthetic peridotite and oxygen fugacity has been successfully established according to the most abundant rocks in the upper mantle at high temperature and high pressure. It is completely consistent with the previous model at atmospheric pressure, which was obtained by Duba and Constable,[35] about the electrical conductivity of lherzolite and oxygen fugacity at 973 K–1473 K and $CO+CO_2$ controlling oxygen pressure (10^{-5} Pa–1 Pa) from the following formula:

$$\begin{aligned}\log_{10}(\sigma) = {} & (0.8596 \pm 0.00337) \times \log_{10} f_{O_2} \\ & - (0.92305 \pm 0.03232).\end{aligned} \tag{8}$$

Although this new technique is applicable to different multi-anvil high-pressure large volume presses, which are based on grain interior electrical conductivity measurement, we can obtain the grain boundary electrical conductivity of natural and synthetic samples if the fixed frequency of the ZPlot program on the Solartron-1260 Impedance/Gain-Phase analyser is reduced enough. By using the new technique, if a solid oxygen buffer with better oxidation and reduction abilities, such as Re+ReO_2 and Cr+Cr_2O_3, are adopted, a new oxygen boundary value of Earth's interior may be successfully obtained. This would be based on the *in-situ* laboratory measurement of the grain interior electrical conductivities of minerals and rocks at both an elevated temperature and pressure.[36−38]

References

[1] Sakamoto D, Yoshiasa A, Yamanaka T, Ohtaka O and Ota K 2002 *J. Phys.: Condens. Matter* **14** 11375

[2] Nover G 2005 *Surv. Geophys.* **26** 593

[3] Dai L D, Li H P, Liu C Q, Su G L and Shan S M 2006 *High Pressure Res.* **26** 193

[4] Dai L D, Li H P, Hu H Y and Shan S M 2008 *J. Geophys. Res.* **113** B12211

[5] Dai L D, Li H P, Deng H M, Liu C Q, Su G L, Shan S M, Zhang L and Wang R P 2008 *J. Phys. Chem. Solids* **69** 101

[6] Dai L D, Li H P, Hu H Y and Shan S M 2009 *Rev. Sci. Instrum.* **80** 033903

[7] Dai L D and Karato S I 2009 *Earth Planet. Sci. Lett.* **287** 277

[8] Dai L D and Karato S I 2009 *Phys. Earth Planet. Int.* **176** 83

[9] Dai L D and Karato S I 2009 *P. Jpn. Acad.* B: *Phys.* **85** 466

[10] Evans R L 2008 *Science* **322** 1338

[11] Ohta K, Hirose K, Ichiki M, Shimizu K, Sata N and Ohishi Y 2010 *Earth Planet. Sci. Lett.* **289** 497

[12] Poe B T, Romano C, Nestola F and Smyth J R 2010 *Phys. Earth Planet. Int.* **181** 103

[13] O'Neill H St C 1987 *Am. Mineral.* **72** 280

[14] Ballhaus C, Berry R F and Green D H 1990 *Nature* **348** 437

[15] Ehlers K, Grove T L, Sisson T W, Recca S I and Zervas D A 1992 *Geochim. Cosmochim. Ac.* **56** 3733

[16] Xie H S, Li H P and Xu J A 1998 *Rev. Sci. Instrum.* **69** 517

[17] Li H P, Xie H S, Guo J, Zhang Y M, Xu Z M and Xu J A 1998 *Geophys. Res. Lett.* **25** 817

[18] Li H P, Xie H S, Guo J, Zhang Y M, Xu Z M and Liu C Q 1999 *J. Geophys. Res.* **104** 29439

[19] McCammon C 2005 *Science* **308** 807

[20] Frost D J and McCammon C 2008 *Ann. Rev. Earth Planet. Sci.* **36** 389

[21] Huang X G, Xu Y S and Karato S I 2005 *Nature* **434** 746

[22] Huang X G, Bai W M, Xu Y S and Karato S I 2005 *Acta Petrol. Sin.* **21** 1743

[23] Karato S I 2008 *Phys. Earth Planet. Int.* **170** 152

[24] Karato S I and Dai L D 2008 *Eos Trans. AGU* **89** DI13C-01

[25] Karato S I and Dai L D 2009 *Phys. Earth Planet. Int.* **174** 19

[26] Will G, Cemič L, Hinze E, Seifert K F and Voigt R 1979 *Phys. Chem. Miner.* **4** 189

[27] Xu Y S, Poe B T, Shankland T J and Rubie D C 1998 *Science* **280** 1415

[28] Xie H S, Zhu W G, Hou W, Zhou W G, Guo J and Xu J A 2002 *J. Phys.: Condens. Matter* **14** 11365

[29] Li H P, Xu L P and Liu C Q 2005 *J. Geophys. Res.* **110** B05203

[30] Chou I M 1978 *Am. Mineral.* **63** 690

[31] Long Y Z, Xiao H M, Chen Z J, Wang M X, Jin A Z and Gu C Z 2004 *Chin. Phys.* **13** 1918

[32] Long Y Z, Chen Z J, Peng H L and Liu Z F 2008 *Chin. Phys.* B **17** 2251

[33] Ichiki M, Baba K, Toh H and Fuji-ta K 2009 *Gondwana Res.* **16** 545

[34] Lü G H, Chen H, Wang X Q, Pang H, Zhang G L, Zou B, Li H J and Yang S Z 2010 *Chin. Phys.* B **19** 085202

[35] Duba A and Constable S 1993 *J. Geophys. Res.* **98** 11885

[36] Holzheid A and O'Neil H St C 1995 *Geochim. Cosmochim. Ac.* **59** 475

[37] Nishihara Y, Shinmei T and Karato S I 2006 *Phys. Earth Planet. Int.* **154** 30

[38] Nishihara Y, Shinmei T and Karato S I 2008 *Am. Mineral.* **93** 831